

Temperature-dependent generalized ellipsometry of the metal-insulator phase transition in low-symmetry charge-transfer salts

Achyut Tiwari, Bruno Gompf, and Martin Dressel^{a)}

1. *Physikalisches Institut, Universität Stuttgart, Pfaffenwaldring 57, 70569 Stuttgart, Germany*

Determining the optical and electronic properties of strongly anisotropic materials with symmetries below orthorhombic remains challenging; generalized ellipsometry is a powerful technique in this regard. Here, we employ Mueller matrix spectroscopic and temperature-dependent ellipsometry to determine the frequency dependence of six components of the dielectric-function tensor of the two-dimensional charge-transfer salt α -(BEDT-TTF)₂I₃ across its metal-insulator transition. Our results offer valuable insights into temperature-dependent changes of the components of the spectroscopic dielectric-function tensor across the metal-insulator transition. This advanced method allows extension to other electronic transitions.

The two-dimensional organic conductor α -(BEDT-TTF)₂I₃ has been subject of keen interest among solid-state physicists for several decades due to its rich variety of electronic properties¹. These properties include a correlation-driven metal-insulator transition², superconductivity³, photo-induced phase transitions⁴, and zero-gap semiconductivity⁵ with massless Dirac-like fermions^{6–8}. The material's intriguing behavior has spurred extensive research aimed at understanding the underlying mechanisms governing its electronic responses. α -(BEDT-TTF)₂I₃ is the prime example among two-dimensional organic conductors, which exhibits a metal-insulator-transition at $T_{CO} = 135$ K². This electronically driven metal-insulator phase transition involves an abrupt change from a metallic state to an insulating state⁹ without any remarkable crystallographic transition^{10,11}. Despite significant progress in understanding the metal-insulator transition in α -(BEDT-TTF)₂I₃ over the last years, the underlying mechanism remains poorly understood on a microscopic scale.

In this regard, spectroscopic ellipsometry has been proven to be an excellent tool to gain deeper insights into microscopic characteristics^{12–14}. However, understanding the microscopic properties using macroscopic measurement becomes rather challenging in α -(BEDT-TTF)₂I₃ due to the low symmetry of the triclinic crystals. In crystals with symmetry lower than orthorhombic, the optical response from various directions tends to mix up, which needs proper analysis to accurately disentangle the contributions from different directions. Generalized ellipsometry has been used to determine the dielectric function of low-symmetry crystals such as α -PTCDA¹⁵, pentacene¹⁶, BiFeO₃¹⁷, CdWO₄¹⁸, Ga₂O₃¹⁹ and K₂Cr₂O₇^{20,21}.

In this letter, we present a comprehensive temperature-dependent study employing generalized ellipsometry to investigate the anisotropic dielectric properties and the charge-order phase transition in α -(BEDT-TTF)₂I₃. In the first step, Mueller matrix (MM) ellipsometry is conducted at room temperature to appropriately address the

anisotropic optical behavior of α -(BEDT-TTF)₂I₃. It allows us to determine the crystal orientation relative to the laboratory frame and extract the real and imaginary parts of the six components of the dielectric-function tensor, including the unit-cell angles. Subsequently, we analyze the temperature-dependent changes in the dielectric functions by applying spectroscopic ellipsometry, revealing the metal-insulator phase transition. The crystal orientation acquired via MM is used in this analysis, since the phase transition is solely driven by effective electronic correlation without breaking crystallographic symmetry. Based on the derived temperature-dependent dielectric functions, we discuss the changes appearing in the various excitations across the metal-insulator transition.

The crystal structure of α -(BEDT-TTF)₂I₃ is triclinic, with alternating conducting donor layers of BEDT-TTF molecules and insulating anions (I₃⁻) along the c -direction^{10,22,23}, as depicted in Fig. 1(a). Due to the low symmetry, the electrical and optical properties are characterized by a small in-plane and a substantial out-of-plane anisotropy²⁴. For crystals with symmetry lower than orthorhombic, the non-orthogonal tilting of the crystallographic axes leads to a non-diagonalizable dielectric tensor of six components for non-magnetic material. In this case, the complex dielectric function is given by the frequency-dependent 3×3 tensor²⁵:

$$\tilde{\epsilon} = \begin{pmatrix} \tilde{\epsilon}_{11} & \tilde{\epsilon}_{12} & \tilde{\epsilon}_{13} \\ \tilde{\epsilon}_{12} & \tilde{\epsilon}_{22} & \tilde{\epsilon}_{23} \\ \tilde{\epsilon}_{13} & \tilde{\epsilon}_{23} & \tilde{\epsilon}_{33} \end{pmatrix}. \quad (1)$$

For these crystals, the optical response depends on the direction of the incident light and the crystal orientation, which necessitates careful treatment to accurately disentangle the different contributions from each direction^{16,26}.

Ellipsometry is a powerful technique to explore the optical properties of isotropic samples and thin films^{27–29}. Generalized ellipsometry is a robust tool to investigate anisotropic materials, including monoclinic and triclinic crystals^{16,21,30–34}. It describes the interaction of electromagnetic waves with anisotropic samples within the Jones- or Mueller-matrix formalism. Here, we use the Stokes vector formalism, which represents the connec-

^{a)} Electronic mail: dressel@pi1.physik.uni-stuttgart.de

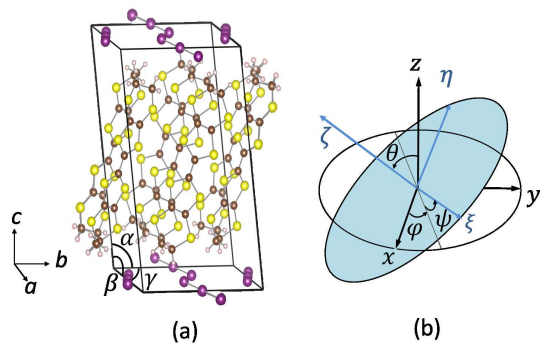


FIG. 1. (a) Unit cell of α -(BEDT-TTF) $_2$ I $_3$. α , β and γ are the triclinic unit-cell angles, and crystallographic axes are indicated as a , b and c ^{10,23}. (b) Schematic representation of the orientation of orthogonal auxiliary frame with respect to laboratory frame (x, y, z) , defined by Euler angles ϕ , θ and ψ .

tion between the real-valued 4×1 Stokes vectors before and after the interaction with the sample using the 4×4 real-valued Mueller matrix^{25,35,36}. The Stokes vector is defined by the experimentally accessible intensities as

$$\mathbf{S} = \begin{pmatrix} S_0 \\ S_1 \\ S_2 \\ S_3 \end{pmatrix} = \begin{pmatrix} I_p + I_s \\ I_p - I_s \\ I_{+45^\circ} - I_{-45^\circ} \\ I_{CR} - I_{CL} \end{pmatrix}. \quad (2)$$

Where $I_p, I_s, I_{+45^\circ}, I_{-45^\circ}, I_{CR}, I_{CL}$ are the intensities of p, s, $+45^\circ$, -45° , and right-, and left-handed circularly polarized light, respectively²⁹. The 4×4 Mueller matrix \mathbf{M} transforms the incident vector \mathbf{S}_{in} to the outgoing vector \mathbf{S}_{out} according to $\mathbf{S}_{out} = \mathbf{M} \mathbf{S}_{in}$. The Mueller matrix elements contain the entire information of the optical response, making it a valuable method for characterizing the complex optical behavior of α -(BEDT-TTF) $_2$ I $_3$.

The investigated α -(BEDT-TTF) $_2$ I $_3$ single crystals were grown via standard electrochemical methods, described in Ref. 37. The compound crystallizes in the space group $P\bar{1}$ ¹⁰. Single crystals are shaped like plates, measuring 3×2 mm in lateral dimensions and with a thickness $67 \mu\text{m}$. Before measurements, the samples were visually inspected under an optical microscope to ensure they were clean and free from defects. Mueller matrix ellipsometry measurements were performed on a state-of-the-art dual rotating compensator ellipsometer (J. A. Woollam RC2), equipped with micro-focus lenses. The experiments with this ellipsometer were carried out at room temperature in the range 300 nm - 1690 nm. The angles of incidence were 55° , 60° , and 65° , while the sample was rotated azimuthally from 0° to 360° in steps of 15° . This comprehensive approach allowed for a thorough characterization of the anisotropic optical properties including the crystallographic orientation.

In order to investigate the dielectric-function tensor of optically anisotropic material, the oriented dipole approach and a more recent general approach that involves

characterizing the dielectric function through the distribution of dipole interactions for each excitation has been employed^{19,21}. Here, for a proper analysis, it is essential to distinguish three coordinate frames: Firstly, the measurements are executed in the laboratory coordinates (x, y, z) , established by the plane of incidence (x, z) and the sample surface (x, y) . Secondly, the macroscopic optical response is characterized by the second-rank tensor of the complex dielectric function $\tilde{\epsilon}$ (eq. 1). Lastly, any microscopic description relies on the electronic system, with axes described by unit vectors \mathbf{x} , \mathbf{y} and \mathbf{z} , the dielectric polarizability \mathbf{P} along $\hat{\mathbf{e}} = \hat{e}_x \mathbf{x} + \hat{e}_y \mathbf{y} + \hat{e}_z \mathbf{z}$ is given by $\mathbf{P}_{\hat{\mathbf{e}}} = \rho_{\hat{\mathbf{e}}}(\hat{\mathbf{e}}\mathbf{E})\hat{\mathbf{e}}$. The complex-valued polarizability functions $\rho_{\hat{\mathbf{e}}}$ may vary with photon energy and must be Kramers-Kronig consistent. The linear polarization response, with n the number of excitations along their respective polarization directions, is given by the superposition:

$$\mathbf{P} = \sum_{l=1}^n \mathbf{P}_{\hat{\mathbf{e}}_l} = \sum_{l=1}^n \rho_{\hat{\mathbf{e}}_l}(\hat{\mathbf{e}}_l \otimes \hat{\mathbf{e}}_l)\mathbf{E} = \chi\mathbf{E}, \quad (3)$$

In the laboratory frame, the macroscopic polarization \mathbf{P} is related to the electric field vector \mathbf{E} by the second-rank dielectric tensor $\tilde{\epsilon}$: $\mathbf{P} = (1 - \tilde{\epsilon})\mathbf{E} = \chi\mathbf{E}$, where χ is the second-rank susceptibility tensor. From the above equations, all the six components of the symmetric dielectric tensor can be deconvoluted. To obtain the microscopic electronic properties from measurements conducted in the laboratory frame, a transformation process is required. The Cartesian coordinate system has to undergo a rotation by the Euler angles ϕ , θ and ψ , transforming it into an auxiliary coordinate system (ξ, η, ζ) [Fig. 1(b)]^{35,38}. For orthorhombic, tetragonal, hexagonal, and trigonal systems, ϕ , θ and ψ can be chosen in a manner that the tensor $\tilde{\epsilon}$ is diagonal in (ξ, η, ζ) . In the case of monoclinic and triclinic systems, complex dielectric tensor $\tilde{\epsilon}$ can not be diagonalize in general.

The six independent components of the dielectric tensor can be extracted by analyzing all ellipsometry data at the same wavelength from multiple azimuth angles and multiple angles of incidence for all energies simultaneously, using a wavelength-by-wavelength approach. Additionally, an independent set of Euler-angle parameters is utilized to describe the orientation of the crystal axes and the elements of the dielectric tensor. In this manner, the spectroscopic dielectric function tensor for triclinic α -(BEDT-TTF) $_2$ I $_3$, represented by the tensor $\tilde{\epsilon}$, is characterized by six components, as shown in Equation 1. In this context, the indices (1,2,3) correspond to the chosen α -(BEDT-TTF) $_2$ I $_3$ system.

In the next step, spectroscopic ellipsometry measurements were performed using a rotating analyzer ellipsometer (J. A. Woollam VASE) equipped with a customized liquid-helium flow cryostat to investigate the temperature-dependent optical properties. The cryostat restricts the angle of incidence to 70° . Window effects were corrected by reference measurements on a silicon

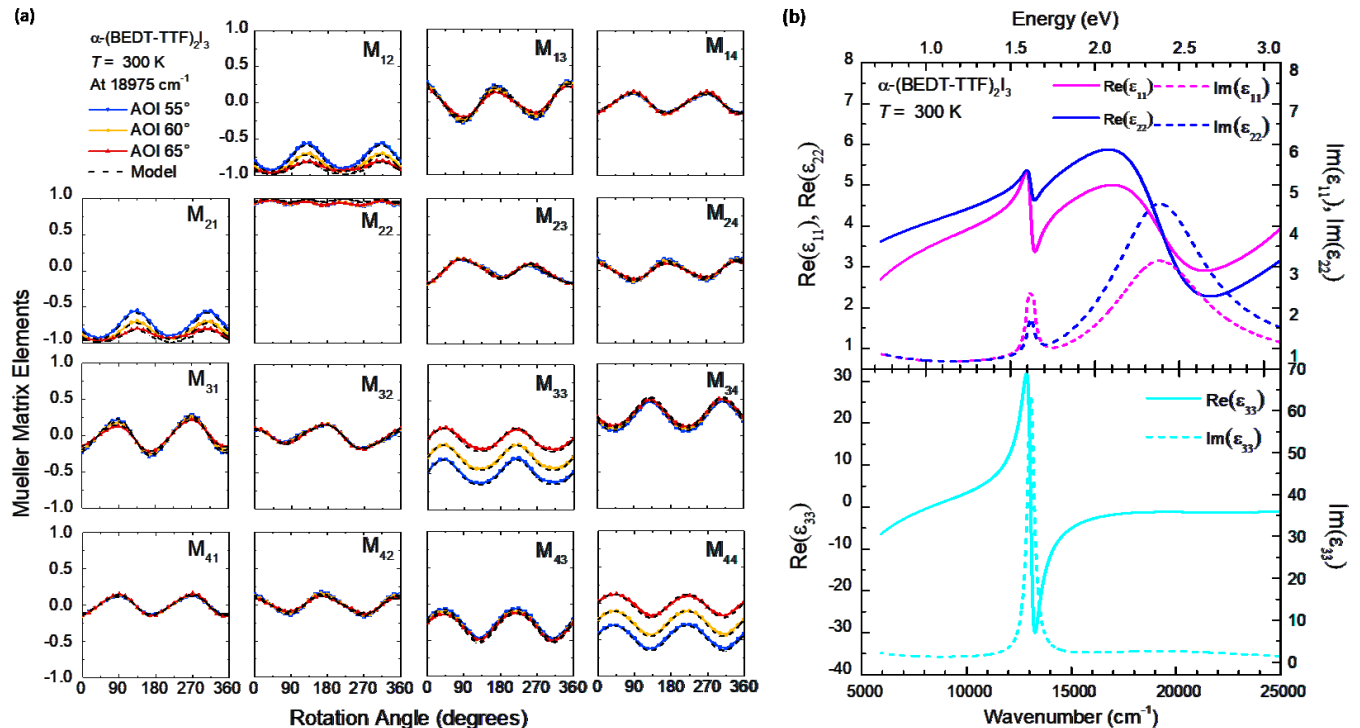


FIG. 2. (a) Experimental (colored solid lines and dots) and best match calculated (black dashed lines) Mueller matrix elements for α -(BEDT-TTF) $_2$ I $_3$ versus sample azimuth rotation at 2.35 eV for three different angles of incidence (55°, 60°, and 65°). The sample was rotated azimuthally from 0° to 360° in steps of 15°. Note all the Mueller matrix elements are normalized to M_{11} . (b) Real (solid lines, left axis) and imaginary (dashed lines, right axis) parts of the dielectric-function tensor ϵ_{11} , ϵ_{22} (upper panel), ϵ_{33} (lower panel) of α -(BEDT-TTF) $_2$ I $_3$. Due to the availability of only one crystal face for measurements, the uncertainty in the out-of-plane components is greater than that of the in-plane components. Nevertheless, the level of sensitivity is adequate to support the conclusion (see supplement document Table-S1).

sample. Only the standard ellipsometry has been performed for temperature-dependent measurement as variable angles of incidence and azimuthal rotations were not feasible due to technical complexities imposed by cryostat and sample. In our analysis, the crystal orientation and optical anisotropy obtained from the Mueller matrix ellipsometry at room temperature could be utilized since no significant structural transition occurs across the metal-insulator transition according to x-ray diffraction measurements^{10,11}. For data analysis, the CompleteEase software by J. A. Woollam Co. Inc. was used.

In order to extract the dielectric functions, all Mueller matrix data were analyzed using a semi-infinite substrate model, representing the properties of α -(BEDT-TTF) $_2$ I $_3$. The possibility of any surface effect can be neglected in the analysis, as the sample surface is perfectly smooth and does not effect the main results. The crystallographic orientation relative to the laboratory frame was precisely determined by fitting the Mueller matrix elements obtained from various angles of incidence and azimuth rotations with a model dielectric function tensor. This model incorporates set of Drude term, Tauc-Lorentz, and Lorentz oscillators, capturing the intricate anisotropic behavior of α -(BEDT-TTF) $_2$ I $_3$. The Drude component

accounts for the contribution of free charge carriers to the dielectric function in metallic states. Tauc-Lorentz and Lorentz oscillators have been employed to characterize intramolecular and intermolecular excitations, respectively, within the visible and near-infrared regions. Pole functions were incorporated to account for the dispersion in the real parts of each tensor element caused by absorption at higher energies beyond the measured spectral range. The oscillators give the Kramers-Kronig consistent dielectric functions. The experimental and simulated Mueller matrix elements exhibited excellent agreement, as depicted in Fig. 2(a), validating the robustness of the fit. The Mueller matrix elements exhibit the approximate symmetry in the off-diagonal elements, corresponding to an antisymmetric Jones matrix. This behavior is generally not expected for triclinic systems but is typical for monoclinic systems⁴⁰. This observation is consistent with the fact that one of the crystal angles, γ , is close to 90°. The parameters of the model dielectric function are summarized in Table-S1. The crystal inclination with respect to the laboratory frame, characterized by the Euler angles, was found to be $\phi = 57.47^\circ \pm 0.27^\circ$, $\theta = 12.08^\circ \pm 0.17^\circ$ and $\psi = 84.04^\circ \pm 0.40^\circ$. The precise orientation is crucial for the analysis and interpretation

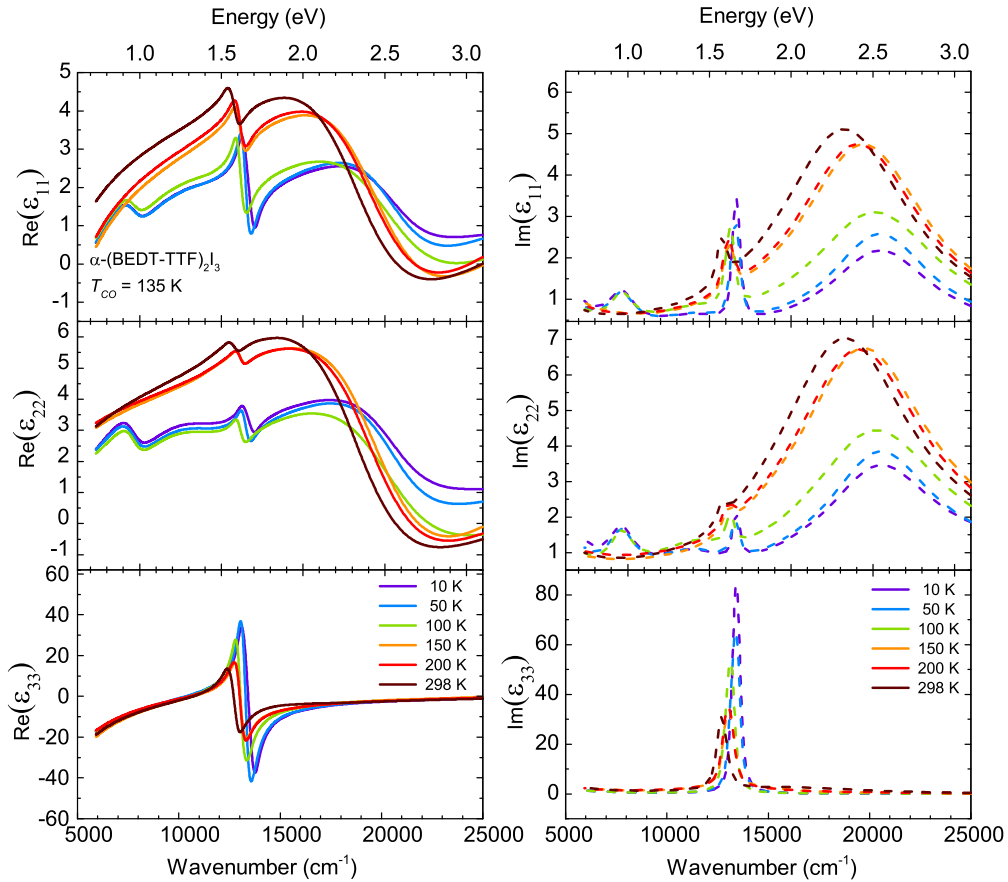


FIG. 3. Real (left panels) and imaginary (right panels) parts of the dielectric functions ϵ_{11} , ϵ_{22} , ϵ_{33} of α -(BEDT-TTF) $_2$ I $_3$ vs frequency, for different temperatures across metal-insulator transition.

of the anisotropic optical response of α -(BEDT-TTF) $_2$ I $_3$.

Fig. 2(b) displays the on-diagonal components of dielectric function tensor at room temperature, as obtained by the Mueller matrix measurements. Notably, in the α -(BEDT-TTF) $_2$ I $_3$ crystal system (a,b,c), on-diagonal components ϵ_{11} , ϵ_{22} , approximately corresponds to in-plane (a,b) dielectric response, whereas ϵ_{33} reflects the out-of-plane (c) dielectric response. The real and imaginary parts of ϵ_{11} , ϵ_{22} , ϵ_{33} revealed intriguing optical properties, exhibiting weak in-plane anisotropy and a pronounced out-of-plane anisotropy. In the a and b -directions, two absorption peaks are observed, with a broad prominent peak at $19,350 \text{ cm}^{-1}$ and a smaller narrower peak at $13,000 \text{ cm}^{-1}$. The overall absorption in the visible spectrum is slightly higher in b -direction and shifts towards lower frequencies when compared to the a -direction. Conversely, the absorption peak at $13,000 \text{ cm}^{-1}$ is more pronounced in the a -direction than in the b -direction. The feature at $19,350 \text{ cm}^{-1}$ can be attributed to intra-molecular excitations, and the peak at $13,000 \text{ cm}^{-1}$ to inter-molecular excitations. The results are in good agreement with Helberg's early study on electronic excitations in α -(BEDT-TTF) $_2$ I $_3$, who reports similar broad and pronounced absorption peaks in

visible range and less pronounced absorption peaks along the a and b -directions^{41–43}. The strongly increased absorption peak at $13,000 \text{ cm}^{-1}$ in c -direction reflects the molecular stacking along that axis, leading to a stronger inter-molecular absorption.

As mentioned, low-temperature measurements were possible only at a single angle of incidence (70°), therefore we are restricted to standard ellipsometric parameters, i.e., Psi and Delta were measured. In the analysis of the temperature-dependent ellipsometric data, different models were employed for the metallic and insulating states. In the metallic state, the analysis incorporates a Drude term, Tauc-Lorentz, and Lorentz oscillators in all three directions. For the insulating state, the Drude term is replaced by a Lorentz oscillator. The experimental data are in excellent agreement with the generated data (see supplement document Fig.-S2), demonstrating the accuracy and suitability of the chosen models. The mean-square error (MSE) and parameters of the model dielectric function are summarized in supplement document, (Table. S2-S7).

Although the crystallographic structure remains unaltered, the temperature-dependent dielectric functions exhibit pronounced changes across the charge-order tran-

sition at 135 K, as shown in Fig. 3. The observed variations are solely caused by effective electronic correlations. In the insulating state, the intra-molecular excitations are weaker and shift towards higher energies in both the a - and b -directions. In contrast, the intermolecular excitations in the a -, b directions are more intense and shift towards higher energies in the insulating state. This effect is even more pronounced in the c -direction, pointing to significant modification in the material's electronic interactions in the stacking direction. While the shifts in the peak positions and the increase of intensities is something to be expected at lower temperatures, the abrupt emergence of a distinct new peak at approximately 7500 cm^{-1} in a - and b -directions in the insulating phase points towards something directly correlated to the metal-insulator transition. Previous results from Yakushi *et al.* suggested that this additional peak might arise from slight structural distortions across the phase transition⁴⁴. These small structural changes seem to be invisible by x-ray diffraction studies^{10,45}. The structural modifications are attributed to alterations of the local anion-molecular interaction which occur when charge ordering sets in. Small displacements of anions lead to variations in the hydrogen bonding between anions and BEDT-TTF molecules, as elucidated by Alemany, Pouget and Canadell^{46,47}. With the help of ellipsometry these slight structural modifications at the metal insulator transition can easily be analyzed. They only happen in the ab -plane, therefore no contribution in the c -direction can be seen, the overall triclinic structure of the crystal remains unchanged.

The here presented comprehensive study on α -(BEDT-TTF)₂I₃ demonstrates that temperature-dependent generalized ellipsometry is a powerful tool for characterizing metal-insulator transitions, even in strongly anisotropic materials. We first employed Mueller matrix ellipsometry at room temperature for a deeper understanding of the optical response of the triclinic crystals. By a detailed analysis of the dielectric functions, we gained valuable insights into the nature of inter-molecular and intra-molecular excitations, observed in the near-infrared and visible spectral regions, respectively. The subsequent temperature-dependent investigations demonstrate the high sensitivity of ellipsometry. While continuous shifts in the peak positions is something to be expected at lower temperatures, the abrupt emergence of a distinct new peak in a - and b -directions in the insulating phase points towards slight structural modifications not identified by x-ray diffraction.

We acknowledge the technical support by Gabriele Untereiner and thank Dieter Schweitzer for providing the crystals. This work is supported by the Deutsche Forschungsgemeinschaft (DFG) under Grant No. DR228/63-1 and GO642/8-1.

SUPPLEMENTARY MATERIAL

See supplementary materials for a list of parameters used to fit the Mueller matrix elements by Drude and various oscillator models. Also shown are spectra of the experimental and calculated Mueller matrix elements at different angles of incidence and for various azimuth rotations in steps of 45° . The room-temperature off-diagonal elements of the dielectric tensor are plotted as a function of frequency. We present the temperature dependent standard ellipsometric parameters and list model parameters of the oscillators used to fit the temperature dependent standard ellipsometric data. Spectra of the off-diagonal elements of the complex dielectric tensor are plotted for different temperatures.

DATA AVAILABILITY

The data that support the findings of this study are available within the article and its supplementary material.

- ¹M. Dressel and S. Tomić, "Molecular quantum materials: electronic phases and charge dynamics in two-dimensional organic solids," *Adv. Phys.* **69**, 1–120 (2020).
- ²T. Takahashi, Y. Nogami, and K. Yakushi, "Charge ordering in organic conductors," *J. Phys. Soc. Jpn.* **75**, 051008 (2006).
- ³N. Tajima, A. Ebina-Tajima, M. Tamura, Y. Nishio, and K. Kajita, "Effects of uniaxial strain on transport properties of organic conductor α -(BEDT-TTF)₂I₃ and discovery of superconductivity," *J. Phys. Soc. Jpn.* **71**, 1832–1835 (2002).
- ⁴S. Iwai, K. Yamamoto, A. Kashiwazaki, F. Hiramatsu, H. Nakaya, Y. Kawakami, K. Yakushi, H. Okamoto, H. Mori, and Y. Nishio, "Photoinduced melting of a stripe-type charge-order and metallic domain formation in a layered BEDT-TTF-based organic salt," *Phys. Rev. Lett.* **98**, 097402 (2007).
- ⁵T. Mori, "Requirements for zero-gap states in organic conductors," *J. Phys. Soc. Jpn.* **79**, 014703 (2009).
- ⁶T. Peterseim, T. Ivek, D. Schweitzer, and M. Dressel, "Electrically induced phase transition in α -(BEDT-TTF)₂I₃: Indications for Dirac-like hot charge carriers," *Phys. Rev. B* **93**, 245133 (2016).
- ⁷N. Tajima, S. Sugawara, M. Tamura, R. Kato, Y. Nishio, and K. Kajita, "Transport properties of massless Dirac fermions in an organic conductor α -(BEDT-TTF)₂I₃ under pressure," *Europhys. Lett.* **80**, 47002 (2007).
- ⁸N. Tajima, S. Sugawara, R. Kato, Y. Nishio, and K. Kajita, "Effect of the zero-mode Landau level on interlayer magnetoresistance in multilayer massless Dirac fermion systems," *Phys. Rev. Lett.* **102**, 176403 (2009).
- ⁹Y. Yue, K. Yamamoto, M. Uruichi, C. Nakano, K. Yakushi, S. Yamada, T. Hiejima, and A. Kawamoto, "Nonuniform site-charge distribution and fluctuations of charge order in the metallic state of α -(BEDT-TTF)₂I₃," *Phys. Rev. B* **82**, 075134 (2010).
- ¹⁰T. Kakiuchi, Y. Wakabayashi, H. Sawa, T. Takahashi, and T. Nakamura, "Charge ordering in α -(BEDT-TTF)₂I₃ by synchrotron x-ray diffraction," *J. Phys. Soc. Jpn.* **76**, 113702 (2007).
- ¹¹T. J. Emge, P. C. W. Leung, M. A. Beno, H. H. Wang, J. M. Williams, M.-H. Whangbo, and M. Evain, "Structural characterization and band electronic structure of α -(BEDT-TTF)₂I₃ below its 135 K phase transition," *Mol. Cryst. and Liq. Cryst.* **138**, 393–410 (1986).

- ¹²M. Hövel, B. Gompf, and M. Dressel, “Dielectric properties of ultrathin metal films around the percolation threshold,” *Phys. Rev. B* **81**, 035402 (2010).
- ¹³I. Voloshenko, F. Kuhl, B. Gompf, A. Polity, G. Schnoering, A. Berrier, and M. Dressel, “Microscopic nature of the asymmetric hysteresis in the insulator-metal transition of VO₂ revealed by spectroscopic ellipsometry,” *Appl. Phys. Lett.* **113**, 201906 (2018).
- ¹⁴I. Voloshenko, B. Gompf, A. Berrier, G. Schnoering, F. Kuhl, A. Polity, and M. Dressel, “Interplay between electronic and structural transitions in VO₂ revealed by ellipsometry,” *J. Vac. Sci. Technol. B* **37**, 061202 (2019).
- ¹⁵M. Alonso, M. Garriga, N. Karl, J. Ossó, and F. Schreiber, “Anisotropic optical properties of single crystalline PTCDA studied by spectroscopic ellipsometry,” *Org. Electron.* **3**, 23–31 (2002).
- ¹⁶M. Dressel, B. Gompf, D. Faltermeier, A. Tripathi, J. Pflaum, and M. Schubert, “Kramers-Kronig-consistent optical functions of anisotropic crystals: generalized spectroscopic ellipsometry on pentacene,” *Opt. Exp.* **16**, 19770–19778 (2008).
- ¹⁷D. Schmidt, L. You, X. Chi, J. Wang, and A. Ruydi, “Anisotropic optical properties of rhombohedral and tetragonal thin film BiFeO₃ phases,” *Phys. Rev. B* **92**, 075310 (2015).
- ¹⁸G. E. Jellison, M. A. McGuire, L. A. Boatner, J. D. Budai, E. D. Specht, and D. J. Singh, “Spectroscopic dielectric tensor of monoclinic crystals: CdWO₄,” *Phys. Rev. B* **84**, 195439 (2011).
- ¹⁹M. Schubert, R. Korlacki, S. Knight, T. Hofmann, S. Schöche, V. Darakchieva, E. Janzén, B. Monemar, D. Gogova, Q.-T. Thieu, R. Togashi, H. Murakami, Y. Kumagai, K. Goto, A. Kuramata, S. Yamakoshi, and M. Higashiwaki, “Anisotropy, phonon modes, and free charge carrier parameters in monoclinic β -gallium oxide single crystals,” *Phys. Rev. B* **93**, 125209 (2016).
- ²⁰S. Höfer, J. Popp, and T. G. Mayerhöfer, “Dispersion analysis of triclinic K₂Cr₂O₇,” *Vib. Spectrosc.* **72**, 111–118 (2014).
- ²¹C. Sturm, S. Höfer, K. Hingerl, T. G. Mayerhöfer, and M. Grundmann, “Dielectric function decomposition by dipole interaction distribution: application to triclinic K₂Cr₂O₇,” *New J. Phys.* **22**, 073041 (2020).
- ²²K. Bender, K. Dietz, H. Endres, H.-W. Helberg, I. Hennig, H. J. Keller, H. Schäfer, and D. Schweitzer, “(BEDT-TTF)₂⁺J₃⁻: A Two-Dimensional Organic Metal,” *Mol. Cryst. Liq. Cryst.* **107**, 45–53 (1984).
- ²³H. Kobayashi, R. Kato, T. Mori, A. Kobayashi, Y. Sasaki, G. Saito, T. Enoki, and H. Inokuchi, “Crystal Structures and Electrical Properties of BEDT-TTF Compounds,” *Mol. Cryst. and Liq. Cryst.* **107**, 33–43 (1984).
- ²⁴T. Ivek, B. Korin-Hamzić, O. Milat, S. Tomić, C. Claus, N. Drichko, D. Schweitzer, and M. Dressel, “Electrodynamical response of the charge ordering phase: Dielectric and optical studies of α -(BEDT-TTF)₂I₃,” *Phys. Rev. B* **83**, 165128 (2011).
- ²⁵M. Born and E. Wolf, *Principles of optics* (Elsevier, 2013).
- ²⁶G. E. Jellison, N. J. Podraza, and A. Shan, “Ellipsometry: dielectric functions of anisotropic crystals and symmetry,” *J. Opt. Soc. Am. A* **39**, 2225–2237 (2022).
- ²⁷P. Drude, “Ueber die Gesetze der Reflexion und Brechung des Lichtes an der Grenze absorbirender Krystalle,” *Ann. Phys.* **268**, 584–625 (1887).
- ²⁸D. Aspnes, “The accurate determination of optical properties by ellipsometry,” in *Handbook of Optical Constants of Solids*, Vol. 1, edited by E. D. Palik (Academic Press, Burlington, 1997) pp. 89–112.
- ²⁹H. Fujiwara, *Spectroscopic ellipsometry: principles and applications* (John Wiley & Sons, 2007).
- ³⁰R. M. A. Azzam and N. M. Bashara, “Application of generalized ellipsometry to anisotropic crystals,” *J. Opt. Soc. Am.* **64**, 128–133 (1974).
- ³¹M. Schubert, B. Rheinländer, J. A. Woollam, B. Johs, and C. M. Herzinger, “Extension of rotating-analyzer ellipsometry to generalized ellipsometry: determination of the dielectric function tensor from uniaxial TiO₂,” *J. Opt. Soc. Am. A* **13**, 875–883 (1996).
- ³²M. Schubert, “Generalized ellipsometry and complex optical systems,” *Thin Solid Films* **313-314**, 323–332 (1998).
- ³³M. Schubert and W. Dollase, “Generalized ellipsometry for biaxial absorbing materials: determination of crystal orientation and optical constants of Sb₂S₃,” *Opt. Lett.* **27**, 2073–2075 (2002).
- ³⁴D. Schmidt, B. Booso, T. Hofmann, E. Schubert, A. Sarangan, and M. Schubert, “Monoclinic optical constants, birefringence, and dichroism of slanted titanium nanocolumns determined by generalized ellipsometry,” *Appl. Phys. Lett.* **94**, 011914 (2009).
- ³⁵H. Tompkins and E. A. Irene, *Handbook of ellipsometry* (William Andrew, Norwich, NY, 2005).
- ³⁶R. M. A. Azzam, “Ellipsometry,” in *Handbook of Optics*, Vol. 2, edited by M. Bass (McGraw-Hill, New York, 1995) 2nd ed., Chap. 27.
- ³⁷K. Bender, I. Hennig, D. Schweitzer, K. Dietz, H. Endres, and H. J. Keller, “Synthesis, structure and physical properties of a two-dimensional organic metal, di[bis(ethylenedithio)tetrathiofulvalene]triiodide, α -(BEDT-TTF)₂I₃,” *Mol. Cryst. and Liq. Cryst.* **108**, 359–371 (1984).
- ³⁸M. Schubert, *Infrared ellipsometry on semiconductor layer structures phonon*. Vol. 209 (Springer, Berlin, 2005).
- ³⁹I.-H. Suh, Y.-S. Park, and J.-G. Kim, “ORTHON: transformation from triclinic axes and atomic coordinates to orthonormal ones,” *J. Appl. Cryst.* **33**, 994 (2000).
- ⁴⁰O. Arteaga, “Useful Mueller matrix symmetries for ellipsometry,” *Thin Solid Films* **571**, 584–588 (2014).
- ⁴¹H. W. Helberg, “Dispersion of the polarizability tensor by inter- and intrastack excitations in organic conductors,” *Mol. Cryst. Liq. Cryst.* **119**, 179–182 (1985).
- ⁴²H. W. Helberg, “Electronic excitations in (BEDT-TTF)-salts,” in *Organic and Inorganic Low-Dimensional Crystalline Materials*, NATO ASI Series B: Physics, Vol. 168, edited by P. Delhaes and M. Drillon (Springer US, New York, NY, 1987) pp. 321–324.
- ⁴³H. W. Helberg, “Electronic excitations in (BEDT-TTF)-salts,” *Ber. Bunsenges. Phys. Chem.* **91**, 899–901 (1987).
- ⁴⁴K. Yakushi, H. Kanbara, H. Tajima, H. Kuroda, G. Saito, and T. Mori, “Temperature dependence of the reflectance spectra of the single crystals of bis(ethylenedithio)tetrathiafulvalenium salts. α -(BEDT-TTF)₃(ReO₄)₂ and α -(BEDT-TTF)₂I₃,” *Bull. Chem. Soc. Jpn.* **60**, 4251–4257 (1987).
- ⁴⁵Y. Nogami, S. Kagoshima, T. Sugano, and G. Saito, “X-ray evidence for structural changes in the organic conductors, α -(BEDT-TTF)₂I₃, α -(BEDT-TTF)₂IBr₂, β -(BEDT-TTF)₂I₃,” *Synth. Metals* **16**, 367–377 (1986).
- ⁴⁶P. Alemany, J.-P. Pouget, and E. Canadell, “Essential role of anions in the charge ordering transition of α -(BEDT-TTF)₂I₃,” *Phys. Rev. B* **85**, 195118 (2012).
- ⁴⁷J.-P. Pouget, P. Alemany, and E. Canadell, “Donor-anion interactions in quarter-filled low-dimensional organic conductors,” *Mater. Horiz.* **5**, 590–640 (2018).